J Mater Sci (2008) 43:1050–1056
DOI 10.1007/s10853-007-2268-4

Synthesis of Ni nanoparticles by hydrolysis of Mg_2Ni

Huabin Wang · Derek O. Northwood

Received: 1 October 2007 / Accepted: 26 October 2007 / Published online: 15 November 2007

Abstract A simple, new method utilizing the hydrolysis of Mg_2Ni has been successfully developed for the synthesis of Ni nanoparticles. The possible growth mechanisms of Ni nanoparticles are discussed. Compared with conventional preparation methods for Ni nanoparticles, this method has the potential to inexpensively produce Ni nanoparticles on a large scale. In addition, the principle of the method could be applied to the synthesis of other transition metal nanoparticles such as Co, Cu, Ag, Au, Pt, and Pd.

Introduction

Nano-scale materials have attracted a great deal of attention for their attractive chemical and physical properties and potential technological application. Ni nanoparticles with a high surface area can be used as catalysts for oil hydrogenation [1], ketone and aldehyde reduction [2], ethylene cracking [3, 4], dissociation of CH_4 [5], steam reforming of methanol [6], hydrothermal gasification of organic compounds [7], synthesis of the carbon nanofibers and nanotubes [8–11], emission control in diesel vehicles [12], and thermal decomposition of ammonium perchlorate (AP) in composite propellants [13].

In addition, as the particle diameter of magnetic materials is reduced to the nano-range, their magnetic domains may change from multiple to single, which is associated with significant changes in their magnetic properties. It is highly desirable to use particles that are magnetically separated from each other, and where the particle size is such that each individual particle can be considered as an elementary magnet [14].

Ni nanoparticles exhibit superparamagnetic behavior above the blocking temperature [15, 16]. Ni nanoparticles have potential application in magnetic drug delivery [17, 18], magnetic and fluorescent tags in biology [19], hypothermic cancer therapy [20], contrast agents in magnetic resonance imaging [21, 22], nano barcodes [23], and nano-metal inks for printing an ultra fine metal circuit pattern with a few microns width on a given substrate [24–26].

There are a variety of techniques for producing pure metal nanoparticles. These techniques essentially fall into three categories: condensation from a vapor, solid-state processes such as milling, and chemical synthesis. Among the chemical synthesis methods, Ni nanoparticles have been prepared by the Raney method [1], microemulsion [27], sol–gel [28], electrochemical deposition [29], reduction of metal-salts [30], chemical vapor deposition [31, 32], hydrothermal reduction [33, 34], thermal decomposition of organometallic compounds [35, 36], and ion-exchange [16].

The synthesis of Ni nanoparticles is, in certain aspects, reaching maturity, and is poised to go to the next level. It is becoming increasingly important to develop methods for scaling up the production of these materials. During our research on the electrochemical properties of the hydrogen storage alloy Mg_2Ni, we found that Mg_2Ni undergoes hydrolysis in water and spontaneously reacts with water to form $Mg(OH)_2$, Ni, and hydrogen. This phenomenon can be utilized to prepare Ni nanoparticles. Compared with many of the previous chemical methods, this particular

H. Wang (✉) · D. O. Northwood
Department of Mechanical, Automotive and Materials Engineering, University of Windsor, N9B 3P4 Windsor, ON, Canada
e-mail: wang14p@uwindsor.ca

method offers a simple and economical route for producing metal nanoparticles on a large scale. The mechanisms of Ni nanoparticle formations are discussed in detail in this article.

Materials and experimental procedures

Arc-melted Mg_2Ni pellets (MPD Technology Corporation, Wyckoff, USA) were used in this study. The chemical analysis of the arc-melted Mg_2Ni pellets (nominal formula: $Mg_{2.35}Ni$) is given in Table 1. The pellets were ball-milled under an argon atmosphere for 2 h, in a laboratory high-energy ball mill SPEX8000 at a speed of 1,200 rpm. The vial was made from tungsten carbide, and was 6.35 cm in diameter and 7.62 cm long. The milling balls, which were 1.27 cm in diameter, were made from 440C*** martensitic stainless steel. The weight ratio of the balls to the Mg_2Ni pellets was about 1:1.

Ten grams of the ball-milled Mg_2Ni particles were immersed in 500 ml of distilled water and stirred for 120 h. The product then was divided into samples A and B. Sample A was used to obtain the solid hydrolysis product through filtering, and drying using a Rotavapor at 60°C. Sample B was used to prepare the Ni nanoparticles. $Mg(OH)_2$ was carefully removed from the hydrolysis product by adding 0.5 M hydrochloric acid. The sample was rinsed thrice using distilled water, then thrice using 99% pure ethanol. The ethanol was evaporated using a Rotavapor at 60°C. Ni particles were obtained.

The phase compositions of the ball-milled Mg_2Ni particles, their hydrolysis product in distilled water, and the Ni nanoparticles were characterized by using a Philips X-ray diffractometer. The morphology of Ni particles (in ethanol, no drying) and the chemical composition in a micro-area were characterized by JEOL 2010 or Philips and FEI Technai 20 transmission electron microscopes equipped with an energy dispersive X-ray analysis system. The size of Ni particles (in water, no drying) was analyzed using a Zetasizer 3000 HS. The specific surface area of Ni nanoparticles was determined by a nitrogen adsorption and desorption method on a Micromeritics ASAP 2010.

Table 1 Chemical composition of the arc-melted Mg_2Ni pellets (wt%)

Elements	Mg	Ni	O	N	C
$Mg_{2.35}Ni$	49.3	50.6	0.042	0.018	0.023

Results

Besides the main Mg_2Ni peaks, some weak Mg diffraction peaks were observed in the XRD pattern for the ball-milled Mg_2Ni-base materials (see Fig. 1a). This result is in agreement with the chemical analysis, which showed that there is 10 wt% surplus Mg in the initial Mg_2Ni pellets (see Table 1).

After the ball-milled Mg_2Ni was immersed in 500 ml of distilled water, there was initially a rapid release of hydrogen bubbles. The release rate of hydrogen bubbles then gradually slowed down. The pH value of the solution, determined using pH papers, rapidly reached a value of 10–11, and remained at that level.

Brucite ($Mg(OH)_2$), Ni, and some very weak Mg_2Ni peaks were observed in the XRD pattern for the hydrolysis product of the ball-milled Mg_2Ni in distilled water (see Fig. 1b). These results indicate that Mg_2Ni had almost totally hydrolyzed into $Mg(OH)_2$ and Ni after being immersed in distilled water for 120 h. The width of Ni peaks was fairly broad, which reflects the crystalline nature of Ni nanoparticles and their extremely small crystallite size. The morphology of the hydrolyzed product of Mg_2Ni is shown in Figs. 2a and b. There are many spread membranes and needle-like rods shown in Fig. 2a. These needle-like rods are rolled-up membranes (see Fig. 2b). The EDS spectrum (see Fig. 3) shows that these membranes contained a large amount of Mg and O, and a small amount of Ni. In addition, these membranes should contain some hydrogen that cannot be detected by EDS. EDS always caused a hole in the membranes due to burning off.

High-resolution TEM image of the membranes (see Fig. 2c) shows that there are many small crystallites in these membranes. The spacing of the lattice fringes ranges from 0.208 to 0.248 nm. The spacings of the (101) planes in $Mg(OH)_2$ and the (111) planes in Ni are 0.2367 and

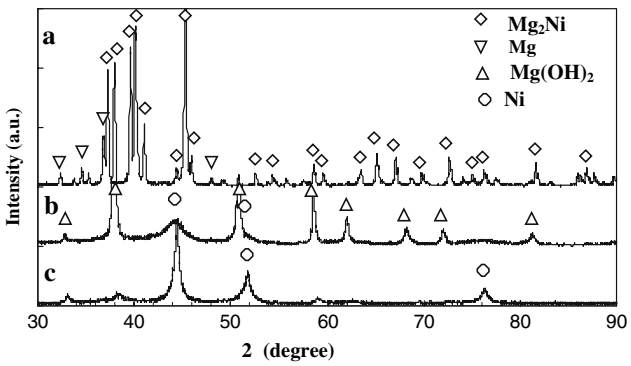

Fig. 1 XRD powder diffraction patterns for (**a**) as-cast Mg_2Ni alloy, (**b**) its hydrolysis product in distilled water for 120 h, (**c**) Ni nanoparticles

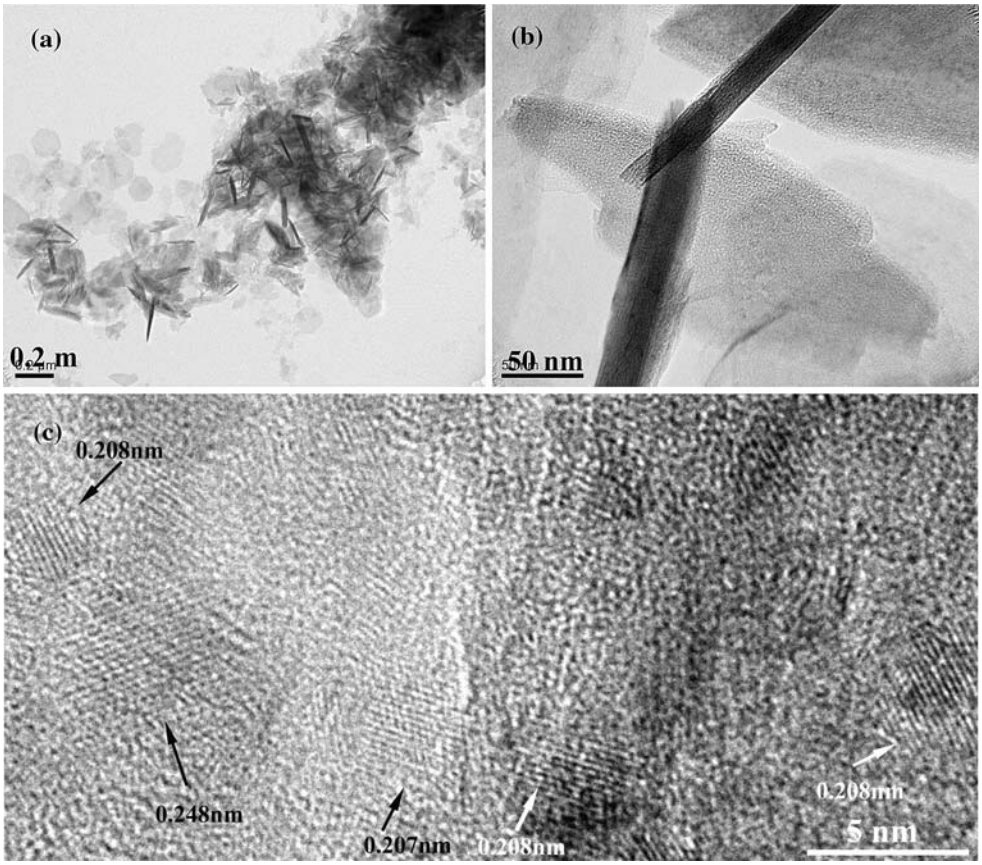

Fig. 2 TEM images of the hydrolysis product of Mg_2Ni (**a**) Low magnification, (**b**) high magnification, (**c**) HRTEM image of the hydrolysis product of Mg_2Ni (membranes)

0.2035 nm, respectively. Therefore, the crystallites with a lattice fringe spacing close to 0.208 nm are from the (111) planes of the Ni nanoparticles and the crystallites with a lattice fringe spacing to 0.248 nm are from the (111) planes of crystalline $Mg(OH)_2$.

Three characteristic peaks can be indexed as the face-centered cubic (fcc) structure of Ni in Fig. 1c, in accordance with the reported XRD data (JCPDS file No. 65-2865).

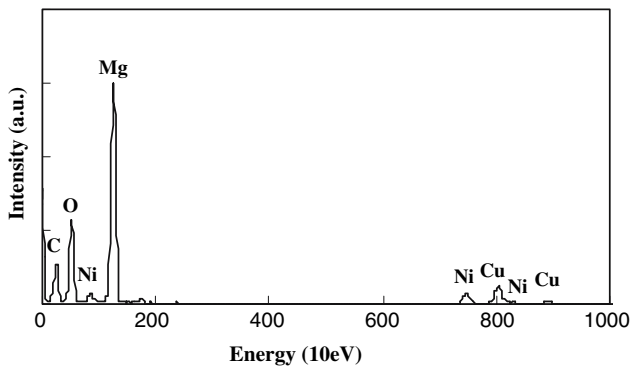

Fig. 3 EDS spectrum of the hydrolysis product of Mg_2Ni (membranes)

Some very small theophrastite ($Ni(OH)_2$) peaks were observed (see Fig. 1c). Since no surfactant was used in these experiments, and the Ni particles resulting from the hydrolysis of Mg_2Ni were very small, the Ni particles generally agglomerated together after they were stored in solution for several days (see Fig. 4a). However, some discrete Ni particles could occasionally be observed (see Fig. 4b). These discrete Ni particles are close to spherical in shape and have a size of about 10 nm. High-resolution TEM image shows that the nanoparticles in Fig. 4c are Ni nanoparticles because the spacing of the lattice fringes was about 0.208 nm. The spacing of the lattice fringes for the particles in Fig. 4d was 0.174 nm, which is close to 0.176 nm (the spacing of the (200) planes in Ni). Five small facets were observed in the inverse fast Fourier transform image at the upper-right corner of Fig. 4d, which suggests that some Ni nanoparticles were polyhedrons.

The result of EDS (see Fig. 5) shows that some Mg and oxygen impurities are present in the Ni nanoparticles. Some of these impurities came from any remaining $Mg(OH)_2$, and some oxygen impurities could come from $Ni(OH)_2$.

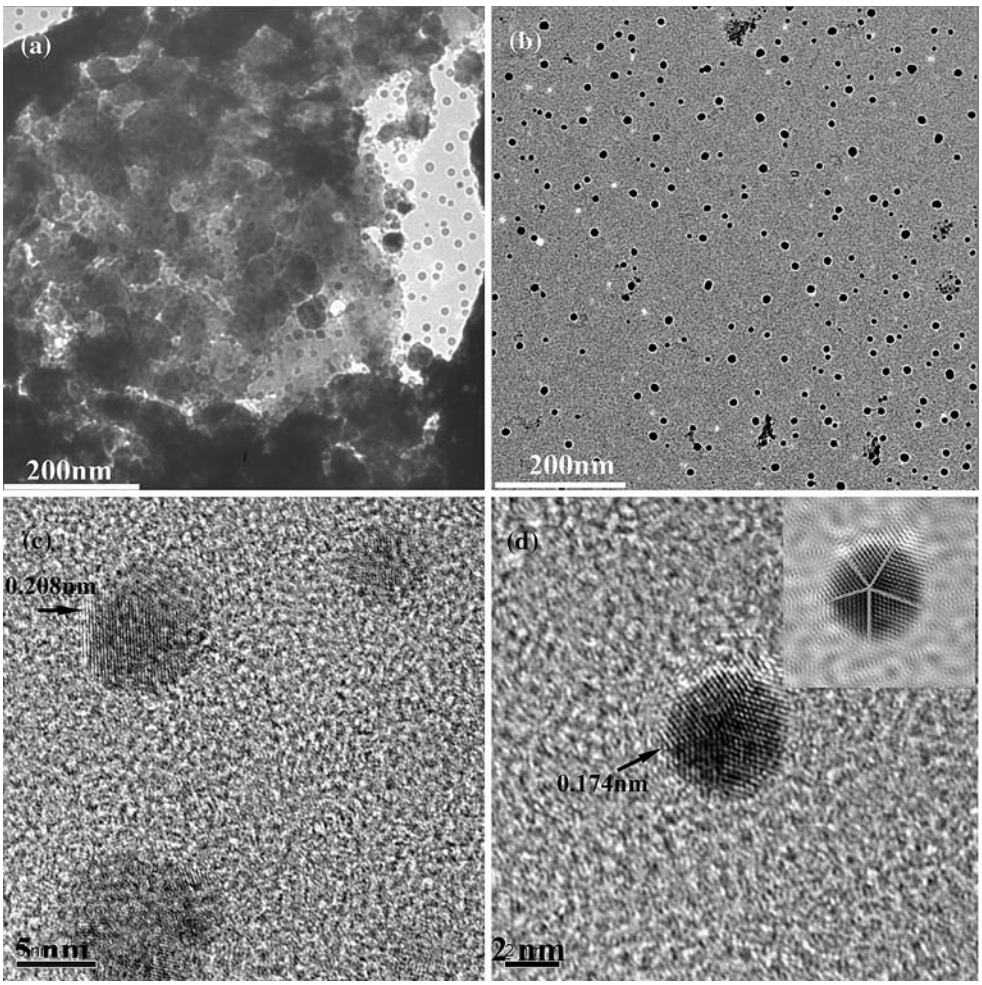

Fig. 4 TEM images of Ni nanoparticles, (**a**) a cluster of Ni nanoparticles, (**b**) discrete Ni nanoparticles, low magnification, (**c**) HRTEM image of individual Ni nanoparticles, (**d**) HRTEM image of individual Ni nanoparticle (corresponding filtered Inverse Fast Fourier Transform image at the upper-right corner)

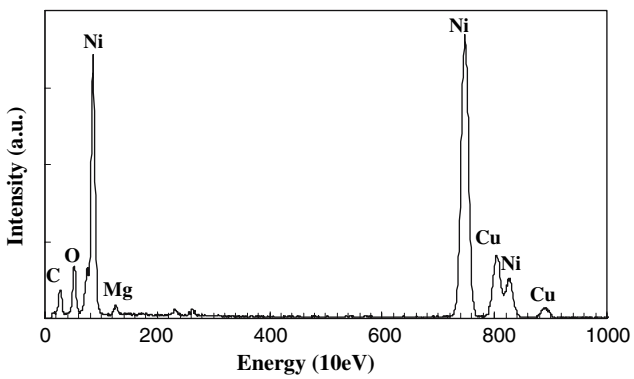

Fig. 5 EDS spectrum of Ni nanoparticles produced by hydrolysis of Mg_2Ni

Figure 6 shows that the particle size of the Ni particles ranged between 7.7 and 24.4 nm. The Ni particles were essentially very small, and roughly mono-dispersed with a mean diameter of 11.7 nm. The nitrogen adsorption and desorption curves for the Ni particles indicate that the specific surface area of the Ni particles is 43.99 m^2/g. The theoretical mean diameter is about 15.3 nm on the basis of the specific surface area if the Ni nanoparticles were assumed to be spherical with the same diameter, which is slightly higher than the mean diameter (11.7 nm).

Discussion

It is well known that Mg particles are chemically very active and can react with water and form $Mg(OH)_2$ thereby releasing hydrogen gas.

The reaction for the hydrolysis of Mg_2Ni, which is less well known, has been given as follows:

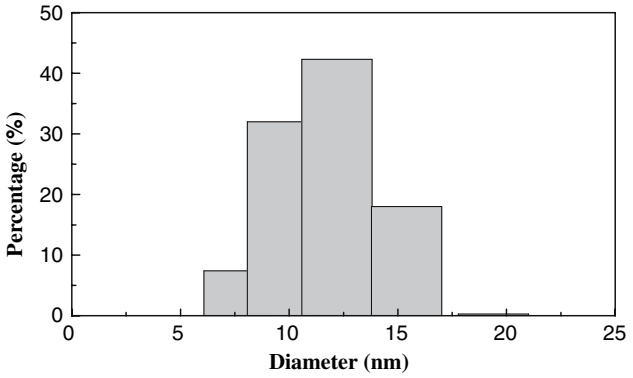

Fig. 6 Particle size distribution of Ni nanoparticles produced by hydrolysis of Mg_2Ni

$$Mg_2Ni(s) + 4H_2O(l) \rightarrow 2Mg(OH_2)(s) + Ni(s) + 2H_2(g) \quad (1)$$

where, s, l, and g in brackets denote the solid, liquid, and gas state, respectively. The standard formation enthalpies and the standard entropies for $Mg(OH)_2$, H_2O, and Mg_2Ni are −924.7 kJ/mol and −149.1 J/°C·mol, −285.53 kJ/mol and 69.95 J/°C·mol, and −51.88 kJ/mol and 94.89 J/°C·mol, respectively. The standard entropies for Ni and H_2 are 29.85 and 130.68 J/°C·mol, respectively [37]. The free energy change for the hydrolysis reaction is given as follows:

$$\Delta G_1 = -544.16\,\text{kJ/mol} + RT\ln\frac{\alpha^2_{Mg(OH)_2}\alpha_{Ni}P^2_{H_2}}{\alpha_{Mg_2Ni}\alpha^4_{H_2O}} \quad (2)$$

The hydrolysis conditions for this study were room temperature, one atmosphere pressure, abundant water, and a limited amount of Mg_2Ni. Therefore, the effect of the activities is neglected, and the free energy change for Reaction 1 can be approximated as the standard free energy change (−544.16 kJ/mol). The thermodynamic analysis thus shows that Mg_2Ni in water spontaneously reacts with the water to form $Mg(OH)_2$, Ni, and hydrogen. The XRD results for the hydrolysis product confirm that the hydrolysis reaction is spontaneous.

The solubility of product constants of $Mg(OH)_2$ is 5.6×10^{-12} [37]. The corresponding pH value is 10.4, which agrees with our experimental results (a pH value of 10–11 in the solution). The addition of an acid to reduce the pH value of the solution during the hydrolysis will accelerate the hydrolysis rate of Mg_2Ni.

Mg is more active than Mg_2Ni. Mg_2Ni will be protected from reaction with water by the hydrolysis of Mg when the ball-milled Mg_2Ni particles were immersed in distilled water. Therefore, the hydrolysis reaction for Mg_2Ni was not initiated until all the Mg was consumed.

Mg_2Ni has a hexagonal structure with $a = 0.519$ nm and $c = 1.322$ nm [38]. The structure is built up by square antiprisms of magnesium that are centered by Ni atoms. The antiprisms are connected via the square faces to columns [38]. Each Ni atom is surrounded by two Ni atoms at a distance of 0.26 nm and eight Mg atoms at a distance of 0.27 nm. Each Mg atom is surrounded by four Ni atoms at a distance of 0.27 nm and 11 Mg atoms at a distance from 0.295 to 0.33 nm [39]. Thus, the larger magnesium atoms form a continuous skeleton, in the voids of which are situated the smaller Ni atoms. Therefore, Mg atoms in the Mg_2Ni compound are still very active.

When Mg_2Ni comes into contact with water, Mg atoms on the surface of Mg_2Ni particles will react with the OH^- ions in water, and form $Mg(OH)_2$. Ni atoms in Mg_2Ni were spontaneously released from the Mg_2Ni. The Ni atoms have a very weak affinity to the excess H^+ ions resulting from the consumption of the OH^- ions. However, the Ni atoms combine together to form Ni nanoparticles under the action of surface energy, and at the same way, the H^+ ions combine together to generate hydrogen gas.

The solubility of $Mg(OH)_2$ in water is very small. The newly formed $Mg(OH)_2$ has to precipitate from water in the vicinity of the Mg dissolution sites. The existence of the $Mg(OH)_2$ particles, and the low mobility of Ni atoms at room temperature, gives rise to the formation of very fine Ni nanoparticles (see Fig. 4). The results of our preliminary experiments indicate that the particle size of Ni nanoparticles prepared by this method was not sensitive to the concentration of Mg_2Ni in aqueous solution.

The high chemical affinity of the magnesium atoms in the Mg_2Ni compound to oxygen leads to the selective oxidation of magnesium, and protects the newly formed Ni nanoparticles from oxidation. Hence, before the Mg_2Ni particles are totally consumed by hydrolysis, the Ni nanoparticles will not oxidize and will have an opportunity to grow in size. After all the Mg_2Ni particles are consumed, the protection of Ni nanoparticles from oxidation will be lost. The Ni nanoparticles could then be oxidized by the dissolved oxygen in the solution. The oxidation reaction is as follows:

$$2Ni(s) + 2H_2O\ (l) + O_2\ (g) \rightarrow 2Ni(OH)_2(s) \quad (3)$$

$Ni(OH)_2$ is a weak alkali. A decrease in the acidity of the solution would be helpful in reducing the oxidation rate of the Ni nanoparticles.

It is generally thought that $Ni(OH)_2$ is formed on the surfaces of Ni nanoparticles because of the oxidation of Ni nanoparticles in the solution. Only very small Ni crystallites (none as large as seen in Fig. 4) were observed in the hydrolysis product. This means that Ni nanoparticles should be growing in size during removal of $Mg(OH)_2$.

The formation of a layer of Ni hydroxide on the surface of the Ni nanoparticles might give rise to a growth arrest of the Ni nanoparticles. Hence, the Ni nanoparticle size is

determined by the temperature and the concentration of the dissolved oxygen.

The oxidation of any Ni nanoparticle prepared by the hydrolysis method requires dissolved oxygen. If there is no dissolved oxygen in solution, Reaction 3 cannot take place. Therefore, if all preparation procedures were carried out in a zero oxygen environment, Ni nanoparticles with low oxygen content could be synthesized by this method.

Besides Ni nanoparticles, other transition metal nanoparticles (Co, Cu, Ag, Au, Rb, and Pd) had been successfully synthesized by our group using this method. The chemical activities of the pure transition metals and the affinity of the elements to hydrogen must be considered. The chemical activities of the pure elements determine whether these nanoparticles can survive both in an aqueous solution and any subsequent dilute acid treatment for the removal of $Mg(OH)_2$. The affinity of the element to hydrogen determines what types of product (pure element nanoparticles or their hydrides) will be generated. If the element has a sufficiently high affinity to hydrogen, hydrides are formed rather than the pure element. For example, the hydrolysis product of Mg_3N_2 and Ca_2C are ammonia (NH_3) and acetylene (C_2H_2), respectively.

The initial materials used in this method can be readily fabricated using a melting–casting method on a large scale. The hydrolysis processing of the metal and magnesium intermetallics, and the removal of $Mg(OH)_2$, can also be scaled up. Therefore, compared with conventional preparation methods of Ni particles, this method has a great potential to economically produce Ni nanoparticles on a large scale.

Conclusions

The main conclusions from this study are as follows:

1. Mg_2Ni spontaneously undergoes hydrolysis in water, and reacts with water to form $Mg(OH)_2$, Ni and hydrogen.
2 The Ni nanoparticles prepared by hydrolysis of Mg_2Ni were spherical in shape (or polyhedrons) with a size of about 10 nm.
3. Compared with conventional preparation methods for Ni nanoparticles, this method has the potential to inexpensively produce Ni nanoparticles on a large scale.
4. The principle of the method could be applied to the synthesis of other transition metal nanoparticles such as Co, Cu, Ag, Au, Pt, and Pd.

Acknowledgements This research was financially supported by the Natural Sciences and Engineering Research Council of Canada (NSERC) through a Discovery Grant awarded to Dr. Derek O. Northwood. The access to facilities, assistance with some experimentation, and critical insights provided by Drs. H. Eichhorn and A. Demenev are greatly appreciated.

References

1. Spencer MS, Twigg MV (2005) Annu Rev Mater Res 35:427
2. Curran DP (1983) J Am Chem Soc 105:5826
3. Vang RT, Honkala K, Dahl S, Vestergaard EK, Schnadt J, Lagsgaard E, Clausen BS, Norskov JK, Besenbacher F (2005) Nat Mater 4:160
4. Daley SP, Utz AL, Trautman TR, Ceyer ST (1994) J Am Chem Soc 116:6001
5. Cui Y, Xu H, Ge Q, Wang Y, Hou S, Li W (2006) J Mol Catal A: Chem 249:53
6. Iwasa N, Masuda S, Takezawa N (1995) React Kinet Catal Lett 55:349
7. Sharma A, Nakagawa H, Miura K (2006) Fuel 85:2396
8. Libera J, Gogotsi Y (2001) Carbon 39:1307
9. Ren Z, Huang Z, Wang D, Wen J, Xu J, Wan J, Calvet LE, Chen J, Klemic JF, Reed MA (1999) Appl Phys Lett 75:1086
10. Cheng H, Li F, Su G, Pan H, He L, Sun X, Dresselhaus MS (1998) Appl Phys Lett 72:3822
11. Kukovecz A, Konya Z, Nagaraju N, Willems I, Tamasi A, Fonseca A, Nagy JB, Kiricsi I (2000) Phys Chem Chem Phys 2:3071
12. Li S, Li B (1996) React Kinet Catal Lett 57:183
13. Jiang Z, Li S, Zhao F, Liu Z, Yin C, Luo Y, Li S (2006) Propel Explo Pyrotech 31:139
14. Voigtlinder B, Meyer B, Amer NM (1991) Phys Rev B 44: 10354
15. Ely TO, Amiens C, Chaudret B, Snoeck E, Verelst M, Respaud M, Broto JM (1999) Chem Mater 11:526
16. Yoon M, Kim Y, Volkov V, Song HJ, Park YJ, Park IW (2005) Mater Chem Phys 91:104
17. Pankhurst QA, Connolly J, Jones SK, Dobson J (2003) J Phys D: Appl Phys 36:R167
18. Tartaj P, Morales MP, Verdaguer SV, Carreno TG, Serna CJ (2003) J Phys D: Appl Phys 36:R182
19. Son S, Reichel J, He B, Schuchman M, Lee S (2005) J Am Chem Soc 127:7316
20. Bettge M, Chatterjee J, Haik Y (2004) Biomagnetic Res Tech 2:4
21. Tanase M, Bauer LA, Hultgren A, Silevitch DM, Sun L, Reich DH (2001) Nano Lett 1:155
22. Mock JJ, Oldenburg SJ, Smith R, Schultz DA, Schultz S (2002) Nano Lett 2:465
23. Nicewarner-Pena SR, Freeman RG, Reiss BD, He L, Pena DJ, Walton ID, Cromer R, Keating CD, Natan MJ (2001) Science 294:137
24. Majima M, Koyama K, Tani Y, Toshioka H, Osoegawa M, Kashihara H, Inazawa S (2002) SEI Tech Rev 54:25
25. Okada I, Shimoda K, Miyazaki K (2006) SEI Tech Rev 62:55
26. Jiang H, Moon K, Lu J, Wong C (2005) J Elect Mater 34:1432
27. Hou Y, Gao S (2003) J Mater Chem 13:1510
28. Fonseca FC, Goya GF, Jardim RF (2002) Phys Rev B 66:104406
29. Whitney TM, Jiang JS, Searson PC (1993) Science 261:1316
30. Chen D, Hsieh C (2002) J Mater Chem 528:2412
31. Park J, Kang E, Son S, Park H, Lee M, Kim J, Kim K (2005) Adv Mater 17:429
32. Carpenter GJC, Wronski ZS (2004) J Nanoparticle Res 6:215
33. Liu Q, Liu H, Han M, Zhu J, Liang Y, Xu Z, Song Y (2005) Adv Mater 17:1995
34. Liu Z, Li S, Yang Y, Peng S, Hu Z, Qian Y (2003) Adv Mater 15:1946

35. Migowsky P, Teixeira SR, Machado G, Alves MCM, Geshev J, Dupont J (2007) J Electron Spectrosc Relat Phenom 156–158:195
36. Migowsky P, Machado G, Teixeira SR, Alves MCM, Morais J, Traverse A, Dupont J (2007) Phys Chem Chem Phys 9:4814
37. Kubascheski O, Alcock CB (1979) Metallurgical thermochemistry, 5th edn, International Series on Mater. Sci. Tech., vol 24. Pergamon Press, Toronto
38. Perminov VP (1967) Poroshkovaya Metallurgiya 5:89
39. Gingl F, Selvam P, Yvon K (1993) Acta Cryst 49B:201